Unified model for cosmic rays above 10^{17} eV and the diffuse gamma-ray and neutrino backgrounds

G. Giacinti,[1,2] M. Kachelrieß,[3] O. Kalashev,[4] A. Neronov,[5] and D. V. Semikoz[6]

[1]*Max-Planck-Institut für Kernphysik, Postfach 10 39 80, 69029 Heidelberg, Germany*
[2]*University of Oxford, Clarendon Laboratory, Oxford OX1 3PU, United Kingdom*
[3]*Institutt for fysikk, NTNU, Trondheim, Norway*
[4]*Institute for Nuclear Research of the Russian Academy of Sciences, Moscow, Russia*
[5]*ISDC, Astronomy Department, University of Geneva, Ch. d'Ecogia 16, Versoix 1290, Switzerland*
[6]*AstroParticle and Cosmology (APC), 10 rue Alice Domon et Léonie Duquet, F-75205 Paris Cedex 13, France*

(Received 29 July 2015; published 28 October 2015)

We investigate how the extragalactic proton component derived within the "escape model" can be explained by astrophysical sources. We consider as possible cosmic ray (CR) sources normal or starburst galaxies and radio-loud active galactic nuclei (AGN). We find that the contribution to the total extragalactic proton flux from normal and starburst galaxies is only subdominant and does not fit the spectral shape deduced in the escape model. In the case of radio-loud AGN, we show that the complete extragalactic proton spectrum can be explained by a single source population, BL Lac/FR I, for any of the potential acceleration sites in these sources. We calculate the diffuse neutrino and γ-ray fluxes produced by these CR protons interacting with gas inside their sources. For a spectral slope of CRs close to $\alpha = 2.1$–2.2 as suggested by shock acceleration, we find that these UHECR sources contribute the dominant fraction of both the isotropic γ-ray background and of the extragalactic part of the astrophysical neutrino signal observed by IceCube.

DOI: 10.1103/PhysRevD.92.083016 PACS numbers: 98.70.Sa, 98.70.Rz, 98.70.Vc

I. INTRODUCTION

The search for the sources of ultrahigh-energy cosmic rays (UHECR) and for an understanding of their acceleration mechanism is one of the important challenges in astroparticle physics. It has been hoped for that CRs at the highest energies would be only weakly deflected in magnetic fields and hence sources could be identified by usual astronomical methods. Both the Pierre Auger Observatory (PAO) and the Telescope Array (TA) do observe anisotropies in the arrival directions of UHECRs [1,2], and a hot spot observed by TA also has a large statistical significance. However, these anisotropies extend over medium angular scales, similar to what was found in Ref. [3] for previous experimental data, and no successful correlation of UHECRs with potential astrophysical sources has been achieved yet. Meanwhile, there has been steady progress in other areas: The all-particle CR spectrum has been measured precisely, and data on the primary composition have become available. In [4] the Auger Collaboration provided constraints on the fraction of four different elemental groups above 6×10^{17} eV, while the KASCADE-Grande experiment covered, with its composition measurements, energies up to 2×10^{17} eV [5]. Although the derived composition depends on the hadronic interaction models used for the analysis, the following qualitative conclusions can be drawn: First, the proton fraction amounts to ∼40%–60% in the energy range between 7×10^{17} eV and 7×10^{18} eV and decreases afterwards, while the fraction of intermediate nuclei (He, N) increases. Second, the iron fraction in the energy range between 7×10^{17} eV and 2×10^{19} eV is limited by $\lesssim$15%–20% and its central value is consistent with zero. Thus, the Galactic contribution to the observed CR spectrum has to die out around 7×10^{17} eV, unless an additional subdominant and heavy Galactic component remains. Neither light nor intermediate elements above this energy can have a Galactic origin because their anisotropy would otherwise overshoot the upper limits set by Auger on the CR dipole anisotropy (see Ref. [6]).

These results provide a strong constraint on models for the transition between the Galactic and the extragalactic CR component. In particular, they exclude the dip model [7] which requires a proton fraction $\gtrsim$90%. In other models, the ankle at $E \approx$ a few $\times 10^{18}$ eV has been identified with the transition between Galactic and extragalactic CRs [8,9]. However, such a high value of the transition energy exaggerates the acceleration problem of Galactic CR sources and contradicts the low iron fraction determined by Auger. Alternatively, it has been suggested that two populations of extragalactic CR sources exist, one dominating below and one above the ankle [10]. Since there exists no convincing model for these two source classes and their properties, a more economical explanation based on a single extragalactic source type is desirable.

Several recent studies tried to explain the measured spectrum and the composition both above and below the ankle using models with a mixed composition [11–13]. Two of them, Refs. [11,12], explain the light composition below the ankle by photo-disintegration in the CR sources, while at higher energies the initial mixed composition survives.

In Ref. [12], the energy spectra of nuclei in the source are assumed to follow a $1/E$ power law. As a result, the extragalactic sources do not contribute at $E \lesssim 3 \times 10^{17}$ eV. In Ref. [11], the original index of nuclei spectra is around 2.1–2.2, as required by acceleration models, but all low-energy nuclei are photo-disintegrated in the sources. As a result, the spectra of nuclei leaving the source are close to a $1/E$ power law, while the proton spectrum follows the original acceleration spectrum because of a decaying neutron component which escapes from the source. These models predict a contribution of extragalactic sources to the proton spectrum in the energy range measured by KASCADE-Grande.

A disadvantage of these types of models is that they predict a negligible contribution from extragalactic CR sources to the observed IceCube neutrino signal. Thus, the extragalactic neutrino flux is disconnected from the extragalactic CR flux, requiring that extragalactic neutrinos are produced in "hidden sources" with a large interaction depth for protons. In both models, sources with strongly positive evolution give the major contribution to the UHECR flux. In contrast, the authors of Ref. [13] study sources with negative evolution in order to explain the composition measured by Auger with softer fluxes $\propto 1/E^2$ without invoking photo-disintegration.

In this work, we investigate which CR source classes can explain the extragalactic proton component derived within the escape model [14,15] and, at the same time, can give a significant contribution to the isotropic γ-ray background (IGRB) measured by Fermi-LAT [16] and to the astrophysical neutrino signal observed by IceCube [17]. These neutrinos have been suggested to have a Galactic (e.g. [18–20]) and/or an extragalactic origin (e.g. [21]), and may have a hadronuclear origin [22–24]. Amongst others, radio-loud AGNs and hosting galaxy clusters have being proposed as possible sources [22], and a connection to $10^{17.5–18.5}$ eV CRs was suggested and investigated in [25]. Secondary neutrinos and γ-ray s from UHECR propagation in clusters were calculated in Ref. [26].

We consider here as possible CR sources normal or starburst galaxies and radio-loud active galactic nuclei (AGN). This choice is motivated by the fact that these sources might give the dominant contribution to the IGRB at low and high energies, respectively. In particular, it has been suggested in Refs. [27] that blazars can contribute up to 100% to the IGRB. As a production mechanism of the secondary γ-ray and neutrino fluxes, we use CR interactions with gas in their sources. We find that normal and star-forming (SF) galaxies can explain neither the spectral shape nor the magnitude of the derived extragalactic proton flux. In the case of radio-loud AGNs, we show that the complete extragalactic proton spectrum can be explained by a single source population. We also calculate the diffuse neutrino and γ-ray fluxes produced by these CR protons interacting with gas. For a spectral slope of CRs close to $\alpha_p = 2.1–2.2$ as suggested by shock acceleration, we find that these UHECR sources can contribute the dominant fraction to the IGRB, and the major contribution to the extragalactic part of the astrophysical neutrino signal observed by IceCube.

II. METHODOLOGY

A. Extragalactic CR proton flux

We summarize first how the extragalactic CR proton flux in the escape model was derived in Ref. [14]. In a first step, we derived the Galactic all-particle CR flux summing up all CR groups obtained for the maximal rigidity $\mathcal{R}_{\rm max} = 10^{17}$ V and accounting for the Auger iron constraint. Then we obtained the total extragalactic flux by subtracting the predicted total Galactic flux from the measured total CR flux. The extragalactic proton flux observed by Auger followed applying the composition measurement [4] where we chose the results obtained using the EPOS-LHC simulation. Finally, we deduced the contribution of extragalactic protons to the observed proton flux by KASCADE and KASCADE-Grande, subtracting from the proton fluxes given in Ref. [5] the prediction of the escape model: Since the predicted Galactic proton flux lies, for energies above $E \gtrsim 3 \times 10^{16}$ eV, below the measured one, the difference has to be accounted for by extragalactic protons. We show in Fig. 1 the deduced extragalactic proton fluxes from KASCADE-Grande and Auger data in the escape model with brown error bars. Combining the KASCADE, KASCADE-Grande and Auger data suggests that the slope of the extragalactic proton energy spectrum is flat at low energies, $E \lesssim 10^{18}$ eV, consistent with $\alpha_p \sim 2.2$, and softens to $\alpha_p \sim 3$ at higher energies, $E \gtrsim 10^{18}$ eV, (cf. Fig. 6).

B. CR interactions with gas and photons

We now summarize how we calculate the interactions of CRs with gas and the extragalactic background light (EBL). We split the propagation into two parts: The first one includes the propagation in the source, the host galaxy and galaxy cluster where we assume that proton interactions with gas are dominant. The spectrum of exiting particles is then used in the second step as an "effective source spectrum" from which we calculate the resulting diffuse flux taking into account the distribution $\rho(z, L)$ of sources as well as the interaction of protons, electrons and photons with the EBL and the CMB. For both steps, we use the open source code [28] which solves the corresponding kinetic

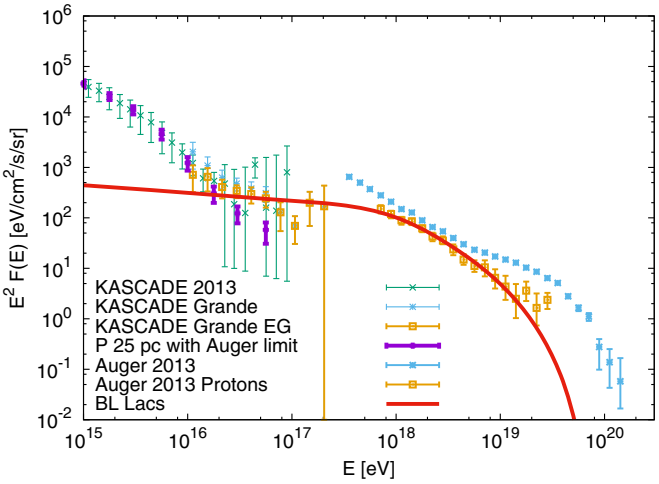

FIG. 1 (color online). Extragalactic proton flux deduced in Ref. [14] within the escape model from KASCADE-Grande and Auger data (brown error bars) together with the original KASCADE and KASCADE-Grande proton data and the total CR flux from Auger. Also shown is the predicted proton flux from BL Lacs (red line).

equations in one dimension. We employ the baseline EBL model of Ref. [29].

As input for the first step, we require the energy dependent grammage $X(E)$ and the proton injection spectrum dN_{CR}/dE. Starting from the injection spectrum of protons, we simulate their propagation and their interaction to obtain the spectra of protons and secondary particles leaving the "effective source." We neglect all interactions except pp interactions in the "effective source." This assumption is not satisfied for some UHECR acceleration sites in the vicinity of the AGN, such as notable acceleration close to the accretion disk where the intense radiation field would make $p\gamma$ interactions dominate over pp. However, for acceleration at the polar caps, the radiation field is sufficiently low for pp to dominate. We also assume that all secondaries escape freely, except electrons. The fate of electrons depends on the strength of the radiation and magnetic fields and on the source size. In extended sources such as galaxies with relatively small magnetic fields, they lose all their energy via synchrotron and inverse Compton radiation. For simplicity, we neglect pair production by photons inside the source, since the following cascade development outside the source leads to a universal spectrum.

The code [28] has been extended implementing pp interactions as follows: The inelastic cross sections $\sigma_{\rm inel}$ of CR nuclei on gas were calculated with QGSJET-II-04 [30]. For the spectrum of secondary photons and neutrinos produced in pp interactions, differential cross sections tabulated from QGSJET-II-04 were used [31]. Secondaries from heavier elements in the CR flux are suppressed. For this reason, we only need to consider the extragalactic CR proton flux in the following, when trying to fit CR, gamma-ray and neutrino fluxes altogether. The contributions from CR nuclei are included, adding a nuclear enhancement factor ε_M. Similarly, the helium component of the interstellar medium was accounted for. Combining both effects, we set $\varepsilon_M = 2.0$ [32]. In order to properly take into account the energy dependence of the grammage, while still using kinetic equations in a one-dimensional framework, we include in the pp interaction rates $R(E)$ the energy dependent grammage $X(E)$. In the case of radio-loud AGNs, we have used, for the grammage, the simple parametrization $X(E) \propto E^{-1/3}$ expected for a turbulent magnetic field with a Kolmogorov spectrum. The normalization was fixed by setting the interaction depth $\tau_{pp} = 1$ at a reference energy $E_{\rm esc}$, which is the only free model parameter in this case. In contrast, for star-forming galaxies, we have used the grammage derived within the escape model (see next section).

III. STAR-FORMING GALAXIES

The escape model developed in Refs. [14,15] provides an excellent description of the measured fluxes of CR nuclei from below the knee to $\sim 10^{18}$ eV. The model predicts an early transition from Galactic to extragalactic CRs. Natural candidate sources for (part of) the extragalactic flux are all other star-forming galaxies (i.e. normal spiral galaxies, starburst galaxies and star-forming AGNs). Moreover, starburst galaxies are expected to give a major contribution to the IGRB, and they have also been considered as possible sources of high-energy neutrinos, assuming they are CR calorimeters (see, amongst others, Refs. [33–36]). Therefore, we first examine how large the contribution from SF galaxies to these fluxes is.

A. CR flux from a single galaxy

We apply the escape model to other normal spiral galaxies. In Refs. [14,15], we argued that a Kolmogorov spectrum for the turbulent galactic magnetic field, together with a $1/E^{2.2}$ power-law injection spectrum, provides an explanation of the knee and of all CR composition measurements between 10^{14} eV and 10^{18} eV. The deviation of the local proton spectrum from this slope is naturally explained by the influence of a local, recent source [37]. Therefore, we use a universal $1/E^{2.2}$ power law as the injection spectrum for all nuclei. Inside galaxies, the spectrum is modified because of energy-dependent CR confinement in them, whereas the CR flux exiting them retains the original injection $1/E^{2.2}$ spectrum. We assume that spiral galaxies have magnetic fields which are, on average, similar to the one in the Milky Way. Hence, we can use, for the confinement time $\tau(E) \propto X(E)$ of CRs in normal spiral galaxies, the grammage $X(E)$ calculated in Refs. [14,15] for the Milky Way.

In contrast, the observed strengths of magnetic fields in starburst galaxies are a factor $\sim$100 larger than in the Milky Way [38]. Since the confinement time $\tau(E)$ is a

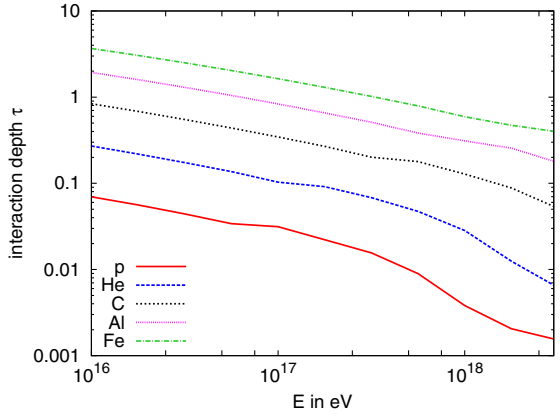

FIG. 2 (color online). Interaction depth τ in a starburst galaxy, as a function of CR energy E, for Fe (top, green line), Al (magenta line), C (black line), He (blue line) and protons (bottom, red line).

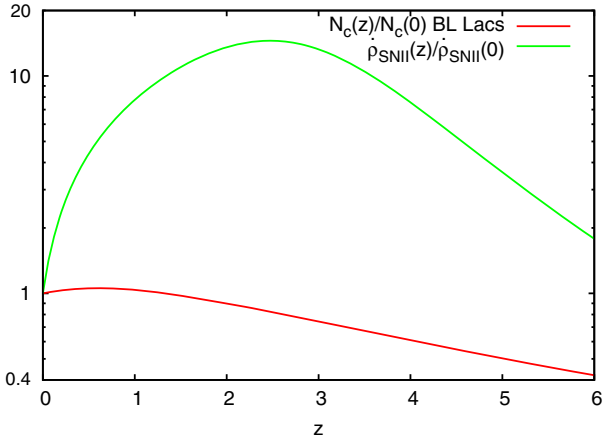

FIG. 3 (color online). Rate $\dot{\rho}$ of type II SNe (green curve) and effective comoving source density $N_c(z)$ of BL Lacs (red line) as a function of redshift, normalized to their present values at $z = 0$.

function of $E/(ZeB)$, we can compensate for this change in B by rescaling the CR energy E in the grammage calculated for the Milky Way. We assume that the coherence length l_c of the turbulent interstellar magnetic fields inside starburst galaxies is not significantly different from that in normal galaxies.

In Fig. 2, we show the resulting interaction depth $\tau = \sigma_{\rm inel} X/m_p$ in a starburst galaxy for various CR nuclei as a function of energy, where we used the density profile described in [15] with $n_0 = 1/{\rm cm}^3$. The fraction of CRs which are absorbed is given by $f_{\rm int} = 1 - \exp(-\tau)$. Thus, the flux of heavy nuclei, such as Al or Fe, leaving a starburst galaxy is exponentially suppressed. In contrast, CR interactions on gas can be neglected in normal galaxies because of their weaker magnetic fields and shorter CR confinement times.

Let us assume that every normal spiral galaxy (resp. every starburst galaxy) accelerates CRs with charge Z up to a maximum energy $E_{\rm max} = Z \times 10^{17}$ eV (resp. $E_{\rm max} = Z \times 10^{18}$ eV). The larger maximum energy achievable in starburst galaxies may e.g. be connected to the larger magnetic fields, which makes an additional acceleration of CRs in superbubbles more efficient [39]. Finally, we assume that the fractions of the injected CR nuclei are the same as the ones below the knee in the Milky Way, except for the proton fraction. We assume that the local proton fraction measured just below the knee is reduced due to the steeper proton spectrum compared to the average one in normal galaxies. We choose to set the proton fraction to $f_p = 0.5$ of the CR flux. Thus, the composition of p:He:N:Al:Fe is fixed as 50:22.5:12.5:5:10, which is consistent with the one deduced in [14] for He:N:Al:Fe at $E = 10^{14}$ eV.

B. Diffuse fluxes from normal spiral and starburst galaxies

We now compute the diffuse flux of extragalactic CRs from all star-forming galaxies. Let us first assume that at redshift z the CR emissivity $Q_{\rm CR}(z)$ scales with the type II supernova (SN) rate $\dot{\rho}_{\rm SNII}(z)$, and thus with the star-formation rate (SFR). This is a phenomenological argument, which does not directly imply that these high-energy CRs have been accelerated at supernova shock waves—see [14] for a discussion on possible acceleration mechanisms. For $\dot{\rho}_{\rm SNII}(z)$, we use the parametrization presented in [40] and take the Baldry & Glazebrook initial mass function [41]. The corresponding type II SN rate is [40]

$$\dot{\rho}_{\rm SNII}(z) = \frac{0.0132(a+bz)h}{1+(z/c)^d}\ {\rm yr}^{-1}\,{\rm Mpc}^{-3}, \qquad (1)$$

with $a = 0.0118$, $b = 0.08$, $c = 3.3$, $d = 5.2$ and $h = 0.7$. It is plotted in Fig. 3 as a green line, which peaks at redshift $z \sim 2$–3. We assume that, globally, a fraction $\epsilon_{\rm CR} = 0.1$ of the kinetic energy of supernovae ($E_{\rm SN} \approx 10^{51}$ erg per SN) is channeled into CRs. The integral CR emissivity $Q_{\rm CR}(z)$ is then

$$Q_{\rm CR}(z) \simeq 9 \times 10^{-22} \frac{(a+bz)h}{1+(z/c)^d} \frac{\rm eV}{{\rm cm}^2\,{\rm s}}. \qquad (2)$$

We define $Q_{\rm CR,SB}$ (resp. $Q_{\rm CR,SP}$) as the integral CR emissivity due to starburst (resp. normal spiral) galaxies. $Q_{\rm CR,SB} = f_{\rm SB} Q_{\rm CR}$ and $Q_{\rm CR,SP} = (1 - f_{\rm SB}) Q_{\rm CR}$, where $f_{\rm SB}$ denotes the fraction of SFR (or supernovae, SNe) occurring in starburst galaxies at redshift z. We parametrize $f_{\rm SB}$ with the two examples proposed in [42]: (i) $f_{\rm SB} = 0.9z + 0.1$ at $z \leq 1$, and $= 1$ otherwise, or (ii) $f_{\rm SB} = 0.1(1+z)^3$ at $z \leq 1$, and $= 0.8$ otherwise. We also consider a scenario (iii) motivated by Ref. [43], where star-forming galaxies are divided into four classes: normal spiral galaxies, starburst galaxies and star-forming AGNs; the latter category is divided into two subsets: SF-AGNs which resemble spiral galaxies and SF-AGNs which resemble starburst galaxies.

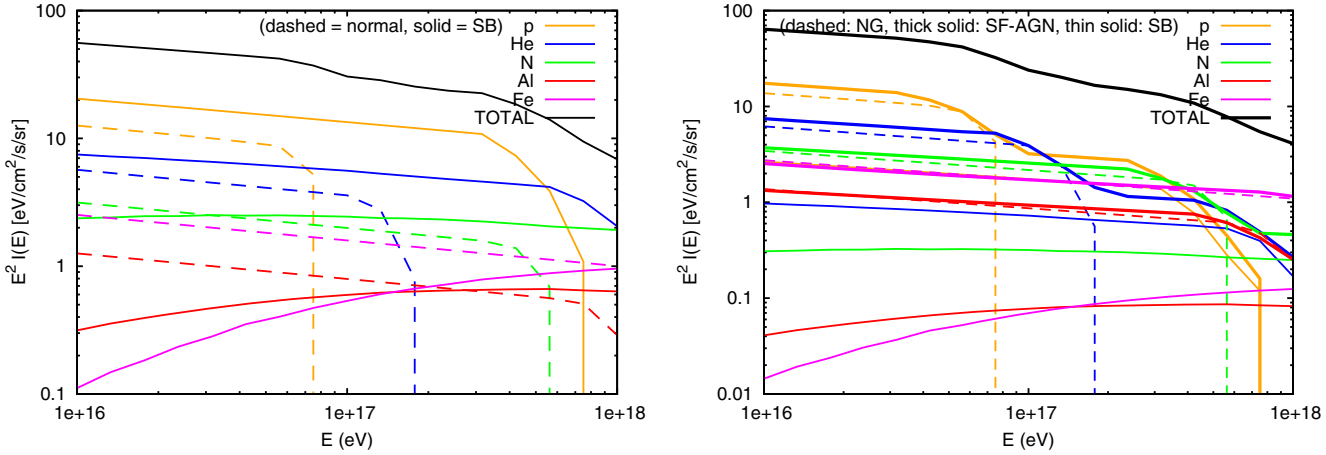

FIG. 4 (color online). Left panel: Diffuse CR flux from normal spiral (dashed lines) and starburst galaxies (solid lines) within scenario (i), as a function of energy. Total flux is shown in black. We show the individual contributions of protons (orange line), He (blue line), N (green line), Al (red line) and Fe (magenta line). Right panel: Diffuse CR flux from normal spirals (dashed lines), star-forming AGNs (thick solid line)—both starburst and nonstarburst ones—and starburst galaxies (thin solid lines) as a function of energy, within scenario (iii). For both panels, we show IGMF with strength $B = 10^{-17}$ G and coherence length $l_c = 1$ Mpc.

We can now determine the differential CR emissivity $q_{\rm CR,SB}(E,z)$ from starburst galaxies, with

$$Q_{\rm CR,SB}(z) = \int dE E q_{\rm CR,SB}(E,z) = \int dE E \dot{n}(z) \frac{dN}{dE}, \quad (3)$$

taking an injection spectrum $\frac{dN}{dE} \propto E^{-2.2}$, between $E_{\rm min} = 1$ GeV and $E_{\rm max} = 10^{18}$ eV. This yields

$$q_{{\rm CR},i}(E,z) \simeq \frac{1\times10^{-20}}{\rm eV\,cm^3\,s} f_i \frac{(a+bz)h}{1+(z/c)^d} \left(\frac{E}{1\ {\rm eV}}\right)^{-2.2}, \quad (4)$$

with $i = \{{\rm SB}, {\rm SP}\}$.

We can find the resulting diffuse CR intensity $I(E)$ from

$$I(E) = \frac{c}{4\pi H_0} \int_0^{z_{\rm max}} \frac{dz}{(1+z)\omega} q_{\rm CR}(z,E') e^{-\tau(E')}, \quad (5)$$

where $\omega = \sqrt{\Omega_\Lambda + \Omega_{\rm m}(1+z)^3}$. In the following, we take $H_0 = 70\ {\rm km\,s^{-1}\,Mpc^{-1}}$, $\Omega_\Lambda = 0.7$ and $\Omega_{\rm m} = 0.3$. Below 10^{18} eV, we can neglect CR interactions in the intergalactic space and thus set $E' = (1+z)E$. For such CR energies, we can neglect absorption during propagation, and τ corresponds to the one given by Fig. 2. The upper integration limit $z_{\rm max}$ is given by the magnetic horizon. In the following, we consider the optimistic case where the intergalactic magnetic fields are sufficiently weak to have $z_{\rm max} \geq 6$ for $E \geq 10^{16}$ eV. This case of no magnetic horizon yields an upper limit on the diffuse extragalactic CR flux one can expect from all star-forming galaxies. We set $\dot{\rho}_{\rm SNII}(z)$ to zero at redshifts $z > 6$, as in [40]. Then,

$$I_{\rm SB}(E) = \frac{c}{4\pi H_0} \times \frac{10^{-20}}{\rm eV\,cm^3\,s} \left(\frac{E}{1\ {\rm eV}}\right)^{-2.2} \times \int_0^{z_{\rm max}} \frac{dz}{\omega} f_{\rm SB}(1+z)^{-3.2} \frac{(a+bz)h}{1+(z/c)^d}.$$

One finds for the total diffuse CR intensity $I(E)$,

$$E^2 I(E) \simeq \frac{1\times10^2\ {\rm eV}}{\rm cm^2\,s\,sr} \left(\frac{E}{10^{15}\ {\rm eV}}\right)^{-0.2}, \quad (6)$$

and $I_{\rm SB}(E) \simeq 0.63 I(E)$ [resp. $I_{\rm SB}(E) \simeq 0.46 I(E)$] in scenario (i) [resp. scenario (ii)]. With $f_p = 0.5$, this gives a CR proton flux that is more than 1 order of magnitude weaker than the extragalactic CR proton flux deduced for the escape model: See the orange line in Fig. 11 of Ref. [14]. This shows that the guaranteed contribution from all star-forming galaxies in the escape model to the diffuse CR flux is negligible. Note that this conclusion does not depend on our assumption about the maximal acceleration energy in star-forming and starburst galaxies.

Using the above parameters, we present in Fig. 4 (left panel) the diffuse fluxes of CR nuclei due to normal and starburst galaxies between $E = 10^{16}$ eV and $E = 10^{18}$ eV. In this computation, we use scenario (i) for the evolution with redshift of the fraction of SNe occurring in starburst galaxies. We consider IGMFs with strength $B = 10^{-17}$ G and coherence length $l_c = 1$ Mpc, e.g. values which are consistent with lower limits from γ-ray observations for time-varying sources [44]. With such parameters, there is no magnetic horizon for any of the nuclei at the energies we consider. The individual contributions of protons and nuclei from normal spiral (resp. starburst) galaxies are shown with the dashed (resp. solid) lines below the total flux. Orange lines are for protons, blue ones are for helium, green ones

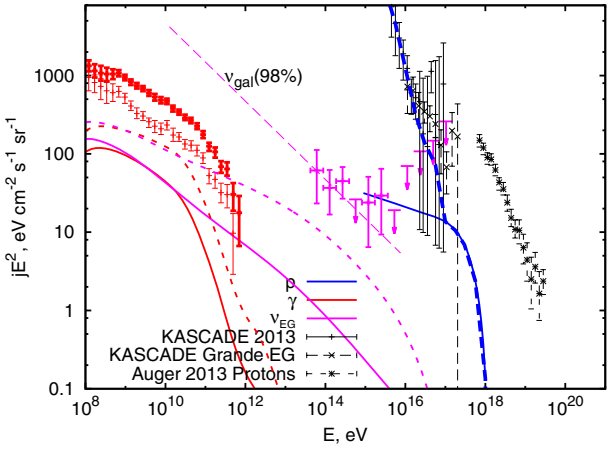

FIG. 5 (color online). Diffuse CR proton (blue lines), gamma-ray (red lines) and neutrino (magenta lines) fluxes from starburst galaxies together with CR proton data from KASCADE, KASCADE-Grande [5] and Auger (black error bars) [4,45], the IGRB and the EGB from Fermi-LAT (red error bars) [16], and high-energy neutrino flux from IceCube (magenta error bars) [17]. Solid red and magenta lines are for gamma-ray and neutrino fluxes with $n = 1$ cm^{-3}, and dashed lines are for $n = 10$ cm^{-3}.

are for CNO nuclei, red ones are for aluminium and magenta ones are for iron. The fluxes of intermediate and heavy nuclei from starburst galaxies are exponentially suppressed at the lowest energies because of the nuclei suffering significant energy losses on background gas in starbursts (see Fig. 2). In Fig. 4 (right panel), we show, for comparison, the results for scenario (iii), where the CR flux is dominated by SF-AGNs.

We consider next the contribution from star-forming galaxies to the diffuse neutrino and γ-ray fluxes. The fraction of CR protons that interact in starburst galaxies is given by $f_{\rm int} = 1 - \exp(-\tau)$, where τ is the interaction depth for protons shown in Fig. 2. We present in Fig. 5 the resulting gamma-ray (red line) and neutrino (magenta) flux from starburst galaxies, within evolution scenario (i). We also plot the diffuse CR proton flux from starburst galaxies. First, we note that star-forming galaxies give a subdominant contribution to the primary CR flux, for the spectral index $\alpha_p = 2.2$ which is favored by the escape model. This discrepancy could be reduced by increasing e.g. the fraction $\varepsilon_{\rm CR}$ of energy transferred to CRs or the SN rate. However, the redshift evolution of star-forming galaxies leads to a proton flux where the spectral shape disagrees with the shape deduced for the extragalactic proton flux. Thus, we conclude that star-forming galaxies cannot be the main contributor to the extragalactic proton flux (up to their $E_{\rm max}$). Next, we compute the secondary neutrino and photon fluxes. We compare them, respectively, to the astrophysical neutrino flux (magenta error bars) measured by IceCube [17] and to the measurement (red error bars) of the extragalactic γ-ray background (EGB) by Fermi-LAT [16]. For the latter, we show both the IGRB (lower curve) and the total EGB including resolved sources (upper curve). Choosing as the average gas density $n = 1/\text{cm}^3$, star-forming galaxies contribute around 30% at 10 GeV to the IGRB, while their contribution to the neutrino signal observed by IceCube reaches 10% below 10^{14} eV. Increasing the gas density by a factor of 10 leads only to an increase of the secondary fluxes by a factor of a few, because the source is already thick in a large energy range. Taking into account the uncertainty in the grammage used, we conclude that star-forming galaxies cannot explain the extragalactic proton flux, but may contribute a significant fraction to the IGRB and to the extragalactic part of the neutrino signal as observed by IceCube, especially at low energies.

Not surprisingly, studies which assume $\alpha_p \simeq 2.0$ and a large grammage in starburst galaxies can reproduce a high-energy neutrino flux comparable to that of IceCube (see e.g. [34,35]).

IV. UHECR SOURCES

We next discuss AGNs, which are generally considered to be prime candidates for the sources of UHECRs. We consider the subset of radio-loud AGN or, more precisely, the BL Lac/Fanaroff-Riley I (FR I) subclass of the radio-loud AGN population. This choice is motivated by two issues: First, the evolution of these sources is relatively slow and peaks at low redshift. Thus, the resulting diffuse CR flux has a rather different spectral shape than the one of star-forming galaxies. Second, BL Lacs have been suggested to be a major contributor to the IGRB (see e.g. [46–48]), which raises the question of whether these sources can also fit, at the same time, the extragalactic CR proton flux expected in the escape model. Also, AGNs are natural candidates of high-energy neutrino sources (see amongst others Refs. [49,50], and Ref. [51] for neutrino production in the inner jets of radio-loud AGNs, including blazars, as sources of UHECRs).

A. Evolution of BL Lacs

We determine the cosmological evolution of BL Lac/FR I sources from the corresponding evolution of the γ-ray luminosity, assuming that the CR and the γ-ray luminosity are proportional,

$$N_c(z) \propto \int_{L_\gamma^{\rm min}}^{L_\gamma^{\rm max}} \rho(z, L_\gamma) L_\gamma dL_\gamma. \tag{7}$$

Here, $\rho(z, L_\gamma)$ is the γ-ray luminosity function (LF), i.e. the number of sources per comoving volume and luminosity. For $\rho(z, L_\gamma)$ we adopt the luminosity-dependent density evolution (LDDE) model of Ref. [47]. Within this model, the LF $\rho(z, L_\gamma)$ can be expressed as

$$\rho(z, L_\gamma) = \rho(L_\gamma) e(z, L_\gamma), \tag{8}$$

with

$$\rho(L_\gamma) = \frac{A}{\log(10) L_\gamma}\left[\left(\frac{L_\gamma}{L_c}\right)^{\gamma_1} + \left(\frac{L_\gamma}{L_c}\right)^{\gamma_2}\right]^{-1}, \quad (9)$$

$$e(z, L_\gamma) = \left[\left(\frac{1+z}{1+z_c(L_\gamma)}\right)^{p_1} + \left(\frac{1+z}{1+z_c(L_\gamma)}\right)^{p_2}\right]^{-1}, \quad (10)$$

and

$$z_c(L_\gamma) = z_c^\star \left(\frac{L_\gamma}{10^{48}\ \mathrm{erg\,s^{-1}}}\right)^{\alpha}. \quad (11)$$

The numerical values for the parameters were determined in [47] from a fit to the statistics of BL Lacs observed by the Fermi-LAT telescope (cf. their Table 3). The evolution of the effective source density with the redshift is shown in Fig. 3. In contrast to average AGNs, the number density of BL Lac and FR I galaxies peaks at low redshift, $z \lesssim 1$. Their evolution is similar to that of galaxy clusters. In fact, most of the FR I sources, which are, in the unified AGN scheme, the same sources as BL Lacs seen under different observation angles, reside in the centers of the dominant central elliptical galaxies of galaxy clusters (cD galaxies).

B. Interactions in BL Lac/FR I sources

We assume that the CR injection spectrum of each source follows a power law with slope α_p and exponential cutoff,

$$\frac{dN_{\mathrm{CR}}}{dE} \propto E^{-\alpha_p} \exp\left(-\frac{E}{E_{\mathrm{cut}}}\right). \quad (12)$$

For each assumed slope α_p of the spectrum, we adjust the cutoff energy E_{cut} in such a way that the spectrum of the entire source population (integrated over redshift) fits best the observed cosmic ray spectrum in the energy range 10^{17} eV–10^{20} eV.

Cosmic rays of low energy are not necessarily escaping from the source. First of all, they could be trapped right in the source. The condition of free escape from the source is that the Larmor radius of the accelerated particle is comparable to the source size R. This condition reads $E \gtrsim E_{\mathrm{free}}$, where

$$E_{\mathrm{free}} \simeq eBR \simeq 3 \times 10^{20}\ \mathrm{eV} \frac{B}{10^4\ \mathrm{G}} \frac{R}{10^{14}\ \mathrm{cm}}. \quad (13)$$

Here, e is electric charge of the particle and B is the magnetic field strength. Lower energy particles are trapped inside the source, be it the AGN central engine, the jet or the radio lobes.

The trapped particles can still escape from the source, but in a diffusive way on a much longer time scale. The details of this process depend on the turbulence of the magnetic field in the relevant source structure. The time scale of turbulence development on a distance scale λ can be estimated by the eddy turnover time $T_{\mathrm{turb}} \sim \lambda/v$, where v is the average bulk velocity of the plasma moving over the distances of the order of λ. In the case of the central engine of AGN, this velocity scale is the typical velocity of the accretion flow that is approximately the Keplerian or free-fall velocity. Close to the black hole horizon, this velocity is relativistic, $v \sim c$. In the AGN jet, the velocity is also $v \sim c$ because the jet is a relativistic outflow. Only in the case of the large scale radio lobes could the velocity be $v \ll c$. In this case it is determined by the details of the interaction of the lobes with the interstellar or intracluster medium. In any case, the eddy turnover scale is certainly much shorter than the source lifetime for all the elements of the radio-loud AGN. This means that the medium and magnetic field in the source are turbulent.

The turbulence power spectrum may, for example, follow a Kolmogorov or an Iroshnikov-Kraichnan power law. In our calculations, we assume that the power spectrum of the turbulence is a Kolmogorov one. Then the escape time of CRs scales with energy as

$$t_{\mathrm{esc}} = \frac{R}{c}\left(\frac{E}{E_{\mathrm{free}}}\right)^{-1/3} \simeq 5 \times 10^6\ \mathrm{s}\left[\frac{E}{10^{11}\ \mathrm{eV}}\right]^{-1/3}, \quad (14)$$

where we used as a source size $R = 10^{14}$ cm and as magnetic field strength $B = 10^4$ G.

Cosmic rays trapped inside the source lose energy by interacting with the ambient medium present in the source. In the case of the accretion flow, the density is moderately low, $n \lesssim 10^{10}\ \mathrm{cm^{-3}}$, for the radiatively inefficient accretion flows powering FR I/BL Lac sources. The energy loss time of CR protons is

$$t_{pp} = \frac{1}{c\kappa\sigma_{pp} n} \simeq 1 \times 10^6\ \mathrm{s}\left(\frac{n}{10^9\ \mathrm{cm^{-3}}}\right)^{-1}, \quad (15)$$

where $\sigma_{pp} \sim (3\text{–}8) \times 10^{-26}\ \mathrm{cm^2}$ is the inelastic pp cross section and $\kappa \simeq 0.6$ the inelasticity. The interaction time is shorter than the escape time, $t_{\mathrm{esc}} \gtrsim t_{pp}$, for CRs with energy $E < E_{\mathrm{esc}} = 8 \times 10^{12}$ eV, where we again used $R = 10^{14}$ cm and $B = 10^4$ G for the numerical estimate. Thus, CRs with energies below ~10 TeV would not escape from the central engine of an AGN powered by a $3 \times 10^8 M_\odot$ black hole. Note, however, that the numerical value of the escape energy depends strongly on the chosen values for n, B and R and should therefore only be considered as an indication.

Our results for the diffuse flux of CR protons from UHECR sources following the BL Lac evolution (9) are shown in Fig. 6 for $E_{\mathrm{cut}} = 10^{19}$ eV, and two different values of CR slope, $\alpha_p = 2.17$ for the upper panel and $\alpha_p = 2.10$ for the middle and lower panels. The Galactic proton flux in the escape model is shown with a dashed

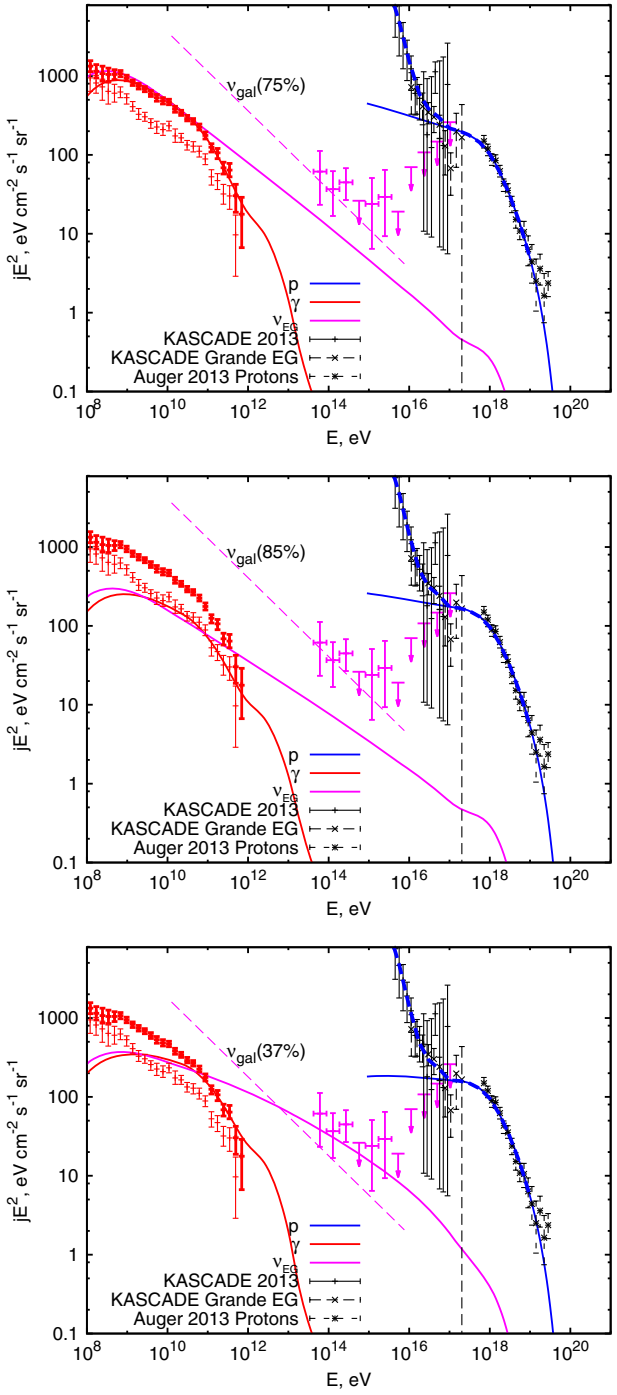

FIG. 6 (color online). Diffuse flux of CR protons from BL Lacs (thick blue line) and Galactic proton flux in the escape model (thin blue line), together with the resulting photon (red line) and neutrino (magenta line) fluxes. Upper panel: $\alpha_p = 2.17$ and $E_{\rm esc} = 3 \times 10^{11}$ eV; middle panel: $\alpha_p = 2.10$ and $E_{\rm esc} = 3 \times 10^{11}$ eV; lower panel: $\alpha_p = 2.10$ and $E_{\rm esc} = 10^{14}$ eV. $E_{\rm max} = 10^{19}$ eV for all three panels. We show CR proton data from KASCADE, KASCADE-Grande [5] and Auger (black error bars) [4,45]. IGRB and EGB from Fermi-LAT (red error bars) [16] and high-energy neutrino flux from IceCube (magenta error bars) [17] are also shown in the figure.

blue line. The choice $\alpha_p = 2.17$ (resp. $\alpha_p = 2.1$) results in an excellent (resp. good) fit of the extragalactic proton component deduced from Auger and KASCADE-Grande measurements.

In the same figure, we also show the secondary fluxes obtained for $E_{\rm esc} = 3 \times 10^{11}$ eV (upper and middle panels) and $E_{\rm esc} = 10^{14}$ eV (lower panel), i.e. values of $E_{\rm esc}$ which are characteristic for CR acceleration close to the supermassive BH powering the BL Lac. The diffuse photon (resp. neutrino) fluxes are shown with red (resp. magenta) lines.

One can see in the upper panel that for $\alpha_p = 2.17$ and $E_{\rm esc} = 3 \times 10^{11}$ eV, the photon flux from the BL Lac/FR I populations may explain the entire extragalactic γ-ray background. This choice of parameters would imply that the main part of the observed TeV γ-ray is of hadronic origin. The synchrotron peak observed in the spectra of BL Lacs at lower energies is caused, in this picture, by electrons which can escape from the central engine and radiate most of their energy in the weaker magnetic field of the surrounding host galaxy. Note that the agreement of the observed and the predicted γ-ray flux is nontrivial, because the model parameters were chosen to fit the UHECR protons, rather than the IGRB spectrum. The predicted high-energy neutrino flux from these AGNs is about a quarter of the IceCube neutrino flux, requiring a Galactic contribution to these neutrinos at the level of 75% (dashed magenta line). The diffuse γ-ray and neutrino fluxes at Earth are due to *in situ* production and cascade emission during CR propagation. We show in the figure both the EGB and the IGRB. One should note that as long as the *in situ* emission dominates, γ-ray s (and neutrinos) point back to their sources and the γ-ray emission is then truly part of the EGB if the source is detected, and not part of the IGRB. If extragalactic magnetic fields have a negligible impact, the distinction would become irrelevant.

For $\alpha_p = 2.1$ and the same grammage (middle panel), the photon and neutrino fluxes are somewhat lower. Indeed, for a CR harder spectrum and for an extragalactic CR flux that satisfies the levels observed at very high energies, less low-energy CRs are present. For $\alpha_p = 2.1$ and $E_{\rm esc} = 3 \times 10^{11}$ eV, the photon flux from the BL Lac/FR I populations provides a good fit to the IGRB deduced by Fermi-LAT [16], as can be seen in the middle panel.

The impact of $E_{\rm esc}$ on the secondary fluxes can be seen by comparing the middle to the lower panel in Fig. 6: For the same slope $\alpha_p = 2.1$, a change in the value of $E_{\rm esc}$ affects the resulting diffuse γ-ray flux much less than the high-energy neutrino flux. The latter are produced by CRs whose interaction depth is $\tau \ll 1$. In this regime, the secondary fluxes scale linearly with the grammage. In contrast, the contribution to the diffuse γ-ray flux of CRs with $\tau \gg 1$ is practically unaffected by a change in $E_{\rm esc}$. For the parameters chosen in the lower panel, one can now explain about ~60% of the IceCube flux by secondary neutrinos from BL Lacs/FR Is.

Explaining the extragalactic CR flux within the escape model, the IGRB/EGB and a large fraction of IceCube neutrinos require a sufficiently large interaction depth at the source (such as that chosen in the lower panel). Therefore, our scenario favors CR acceleration close to the black hole of the BL Lacs/FR Is, in a region where pp interactions dominate over $p\gamma$ interactions, such as the polar caps. Let us, however, note that other sites of CR acceleration such as the jets or lobes of BL Lacs/FR Is can still explain the IGRB/EGB flux, provided that α_p is somewhat larger than 2.2. In this case, the contribution of these sources to the IceCube neutrino flux would, however, be reduced.

C. Neutrinos from BL Lacs and IceCube neutrinos

A remarkable feature of the secondary spectra is that the neutrino flux for our reference parameters can be comparable to the flux of astrophysical neutrinos measured by IceCube [17] [see especially Fig. 6 (lower panel)]. In Fig. 6, the dashed magenta lines indicate the Galactic neutrino flux required[1] to match the observed IceCube signal: The additional Galactic neutrino contribution varies between $\simeq$90% and $\simeq$30%, depending on the value of α_p. This is in line with the results from Refs. [18], which found a high-energy neutrino flux from our Galaxy at the level of ~50% of the IceCube flux, taking a global Galactic cosmic ray spectrum slope of 2.5 instead of 2.7 (local flux).

Also, the slope of our neutrino spectrum is close to the one measured by IceCube. The slope of the extragalactic neutrino spectrum in the IceCube range is $\alpha_\nu \simeq \alpha_p + \delta \simeq$ 2.4–2.5 for an injection spectrum with $\alpha_p \simeq 2.1$–2.2 and Kolmogorov turbulence $\delta = 1/3$. This is an important difference with respect to other models that predict a harder spectrum, with slopes $\approx$2.0, i.e. similar to the slope of the injection spectrum of CRs at the sources. In such models, either the parent CRs escape freely from the sources or lose all their energy in the sources. In our model, CRs diffuse in the source before escaping, which results in an additional softening by δ of the neutrino slope.

Therefore, our model can explain the entire astrophysical neutrino signal observed by IceCube, both in terms of the flux level (Galactic and extragalactic contributions of the same order of magnitude) and of the slope.

The increasing size of the neutrino sample with time will allow IceCube to constrain the ratio of the Galactic and extragalactic high-energy neutrino fluxes, studying the anisotropy of their arrival directions. Within our model, this flux ratio depends strongly on the slope of the extragalactic proton flux and therefore provides important information on the extragalactic UHECR sources.

[1]We estimate the required Galactic contribution assuming an $E^{-2.5}$ spectrum of the Galactic neutrino flux and normalizing the total neutrino flux using the first energy bin of the IceCube data at 6×10^{13} eV.

D. Interactions in the host galaxy and galaxy cluster

We verify, in this subsection, what impact the host galaxy and galaxy cluster have on the diffuse CR proton flux that effectively escapes from them, and on the production of secondaries. Our main conclusions are that only CR protons with energies $E \lesssim 10^{16}$ eV are confined in galaxy clusters and that they only produce a negligible amount of secondary γ-ray and neutrinos. Therefore, the diffuse CR proton flux above $\sim 10^{16}$ eV as well as the diffuse γ-ray and neutrino fluxes we computed previously (see e.g. Fig. 6) are not affected.

Let us first consider the possibility that CRs residing in a kpc scale jet interact with the interstellar medium of the AGN host galaxy. The energy loss time t_{pp} for the typical ISM density $n \sim 1$ cm^{-3} is about 3×10^7 yr, which is longer than the escape time [see Eq. (15)], even for GeV CRs. Thus, CRs in the kpc scale jet escape into the interstellar medium of the source host galaxy, rather than release their energy inside the jet.

The density of the intracluster medium spread over the Mpc scale of the radio lobes still has lower density $n \sim 10^{-2}$–10^{-4} cm^{-3}, so the pp energy loss time is comparable to or longer than the age of the Universe. CRs residing in the radio lobes then escape into the host galaxy cluster of the source, rather than dissipate their energy in the lobes.

Therefore, CRs produced in the AGN jet or in the radio lobes escape in the host galaxy and galaxy cluster. For a magnetic field strength of $B \sim 1$ μG, which is typical for galaxy clusters within a Mpc region, the escape time of the very and ultrahigh-energy CRs contributing to the extragalactic proton flux at Earth (above $\sim 10^{16}$ eV) is small compared to the age of the Universe.

Lower energy cosmic rays produced by an UHECR source which operates only a limited time ($\sim 10^8$ yrs in the case of radio-loud AGNs) are still found in the cluster long after the UHECR source has ceased to exist. Part of their energy will be released while residing in the host galaxy and galaxy cluster. Calculating $E_{\rm esc}$ for the case of the host galaxy cluster, one finds that relativistic particles do not escape for $n \sim 10^{-4}$ cm^{-3}. Host galaxies and galaxy clusters are therefore expected to give only a subdominant contribution to the diffuse neutrino flux. As discussed above, the diffuse γ-ray flux is less sensitive to the value of $E_{\rm esc}$, and pp interactions in the host galaxy may contribute to the IGRB depending on the slope α_p.

V. CONCLUSIONS

We have found that star-forming galaxies (normal spiral galaxies, starburst galaxies and SF-AGNs) give only a subdominant contribution to the high-energy CR flux ($E \lesssim 10^{18}$ eV). Their overall luminosity, their redshift evolution, which peaks at $z \sim 2$–3, and their maximal energy disfavor this source class as the main source of

extragalactic CRs up to the ankle. The resulting secondary fluxes are more uncertain, since they depend on the not-well-determined grammage CRs cross in their host galaxies and galaxy clusters. Even keeping the grammage as a free parameter, it is not possible to explain at the same time a large contribution to the IGRB and to the IceCube neutrinos or to the extragalactic part of the IceCube neutrino signal.

In contrast, we have shown that the BL Lac/FR I population as a source for extragalactic CRs can explain in a unified way the observations of both primary and secondary fluxes. The main reason for this difference with star-forming galaxies or other sources is that the number density of BL Lac and FR I galaxies peaks at low redshift, $z \lesssim 1$.

More precisely, we found that the extragalactic CR proton flux can be explained for any acceleration site (close to the black hole, in the jets or in the lobes) of the BL Lacs/FR I galaxies. However, only acceleration close to the black hole (especially at the polar caps—see Sec. II B) satisfies the required conditions to produce secondary γ-ray and neutrino fluxes that can explain the extragalactic IceCube neutrino flux and the IGRB. For a spectral slope of CR protons close to $\alpha_p = 2.2$, as suggested by shock acceleration and the escape model, we find that such UHECR sources provide the dominant fraction of both the isotropic γ-ray background and of the extragalactic part of the astrophysical neutrino signal observed by IceCube.

We showed that the difference in the slopes of the proton and the neutrino fluxes can be explained by the diffusion of primary protons in the turbulent magnetic field of CR sources. In the case of Kolmogorov turbulence, the power law of the secondary neutrino spectrum is changed by $1/3$, which explains the relatively soft neutrino spectrum with $\alpha_\nu \simeq 2.5$ observed by IceCube using a proton spectrum with $\alpha_p \simeq 2.1$–2.2. This mechanism is universal and does not depend on the type of sources.

ACKNOWLEDGMENTS

G. G. acknowledges funding from the European Research Council under the European Community's Seventh Framework Programme (FP7/2007–2013)/ERC Grant Agreement No. 247039. The work of D. S. was supported in part by RFBR Grant No. 13-02-12175-ofi-m. The numerical calculations have been performed on the computer cluster of the Theoretical Physics Division of the Institute for Nuclear Research of the Russian Academy of Sciences with support by the Russian Science Foundation, Grant No. 14-12-01340.

[1] A. Aab *et al.* (Pierre Auger Collaboration), Astrophys. J. **804**, 15 (2015).
[2] R. U. Abbasi *et al.* (Telescope Array Collaboration), Astrophys. J. **790**, L21 (2014).
[3] M. Kachelrieß and D. V. Semikoz, Astropart. Phys. **26**, 10 (2006).
[4] A. Aab *et al.* (Pierre Auger Collaboration), Phys. Rev. D **90**, 122006 (2014).
[5] W. D. Apel *et al.* (KASCADE-Grande Collaboration), Astropart. Phys. **47**, 54 (2013).
[6] G. Giacinti, M. Kachelrieß, D. V. Semikoz, and G. Sigl, J. Cosmol. Astropart. Phys. 07 (2012) 031; P. Abreu *et al.* (Pierre Auger Collaboration), Astrophys. J. **762**, L13 (2012).
[7] V. Berezinsky, A. Z. Gazizov, and S. I. Grigorieva, Phys. Rev. D **74**, 043005 (2006); V. S. Berezinsky, S. I. Grigorieva, and B. I. Hnatyk, Astropart. Phys. **21**, 617 (2004); R. Aloisio, V. Berezinsky, P. Blasi, A. Gazizov, S. Grigorieva, and B. Hnatyk, Astropart. Phys. **27**, 76 (2007).
[8] C. T. Hill, D. N. Schramm, and T. P. Walker, Phys. Rev. D **34**, 1622 (1986); J. P. Rachen, T. Stanev, and P. L. Biermann, Astron. Astrophys. **273**, 377 (1993).
[9] D. Allard, E. Parizot, and A. V. Olinto, Astropart. Phys. **27**, 61 (2007).
[10] R. Aloisio, V. Berezinsky, and A. Gazizov, Astropart. Phys. **34**, 620 (2011).
[11] N. Globus, D. Allard, and E. Parizot, Phys. Rev. D **92**, 021302 (2015).
[12] M. Unger, G. R. Farrar, and L. A. Anchordoqui, arXiv: 1505.02153 [Phys. Rev. D (to be published)].
[13] A. M. Taylor, M. Ahlers, and D. Hooper, Phys. Rev. D **92**, 063011 (2015).
[14] G. Giacinti, M. Kachelrieß, and D. V. Semikoz, Phys. Rev. D **91**, 083009 (2015).
[15] G. Giacinti, M. Kachelrieß, and D. V. Semikoz, Phys. Rev. D **90**, R041302 (2014).
[16] M. Ackermann *et al.* (Fermi-LAT Collaboration), Astrophys. J. **799**, 86 (2015).
[17] M. G. Aartsen *et al.* (IceCube Collaboration), Phys. Rev. Lett. **113**, 101101 (2014); Phys. Rev. D **91**, 022001 (2015).
[18] A. Neronov, D. V. Semikoz, and C. Tchernin, Phys. Rev. D **89**, 103002 (2014); A. Neronov and D. Semikoz, Astropart. Phys. **72**, 32 (2016).
[19] A. M. Taylor, S. Gabici, and F. Aharonian, Phys. Rev. D **89**, 103003 (2014).
[20] D. B. Fox, K. Kashiyama, and P. Meszaros, Astrophys. J. **774**, 74 (2013).
[21] M. Ahlers and F. Halzen, Phys. Rev. D **90**, 043005 (2014).
[22] K. Murase, M. Ahlers, and B. C. Lacki, Phys. Rev. D **88**, 121301 (2013).
[23] M. Ahlers and K. Murase, Phys. Rev. D **90**, 023010 (2014).

[24] P. Padovani, M. Petropoulou, P. Giommi, and E. Resconi, Mon. Not. R. Astron. Soc. **452**, 1877 (2015).
[25] K. Murase, S. Inoue, and S. Nagataki, Astrophys. J. **689**, L105 (2008).
[26] K. Kotera, D. Allard, K. Murase, J. Aoi, Y. Dubois, T. Pierog, and S. Nagataki, Astrophys. J. **707**, 370 (2009).
[27] F. W. Stecker and M. H. Salamon, Astrophys. J. **464**, 600 (1996); F. W. Stecker and T. M. Venters, Astrophys. J. **736**, 40 (2011); A. Neronov and D. V. Semikoz, Astrophys. J. **757**, 61 (2012).
[28] O. E. Kalashev and E. Kido, J. Exp. Theor. Phys. **120**, 790 (2015).
[29] Y. Inoue, S. Inoue, M. A. R. Kobayashi, R. Makiya, Y. Niino, and T. Totani, Astrophys. J. **768**, 197 (2013).
[30] S. Ostapchenko, Phys. Rev. D **77**, 034009 (2008); **83**, 014018 (2011).
[31] M. Kachelrieß and S. Ostapchenko, Phys. Rev. D **86**, 043004 (2012); **90**, 083002 (2014).
[32] M. Kachelrieß, I. V. Moskalenko, and S. S. Ostapchenko, Astrophys. J. **789**, 136 (2014).
[33] A. Loeb and E. Waxman, J. Cosmol. Astropart. Phys. 05 (2006) 003.
[34] R. Y. Liu, X. Y. Wang, S. Inoue, R. Crocker, and F. Aharonian, Phys. Rev. D **89**, 083004 (2014).
[35] I. Tamborra, S. Ando, and K. Murase, J. Cosmol. Astropart. Phys. 09 (2014) 043.
[36] L. A. Anchordoqui, T. C. Paul, L. H. M. da Silva, D. F. Torres, and B. J. Vlcek, Phys. Rev. D **89**, 127304 (2014).
[37] M. Kachelrieß, A. Neronov, and D. V. Semikoz, arXiv: 1504.06472 [Phys. Rev. Lett. (to be published)]; V. Savchenko, M. Kachelrieß, and D. V. Semikoz, Astrophys. J. Lett. **809**, L23 (2015).
[38] B. C. Lacki and R. Beck, Mon. Not. R. Astron. Soc. **430**, 3171 (2013).
[39] A. Bykov and I. Toptygin, Astron. Lett. **27**, 625 (2001); E. Parizot, A. Marcowith, E. van der Swaluw, A. M. Bykov, and V. Tatischeff, Astron. Astrophys. **424**, 747 (2004); M. Ackermann *et al.*, Science **334**, 1103 (2011).
[40] A. M. Hopkins and J. F. Beacom, Astrophys. J. **651**, 142 (2006).
[41] I. K. Baldry and K. Glazebrook, Astrophys. J. **593**, 258 (2003).
[42] T. A. Thompson, E. Quataert, E. Waxman, and A. Loeb, arXiv:astro-ph/0608699.
[43] C. Gruppioni *et al.*, Mon. Not. R. Astron. Soc. **432**, 23 (2013).
[44] K. Dolag, M. Kachelrieß, S. Ostapchenko, and R. Tomas, Astrophys. J. **727**, L4 (2011); A. M. Taylor, I. Vovk, and A. Neronov, Astron. Astrophys. **529**, A144 (2011).
[45] A. Aab *et al.* (Pierre Auger Collaboration), Braz. J. Phys. **44**, 560 (2014).
[46] A. Neronov and D. V. Semikoz, Astrophys. J. **757**, 61 (2012).
[47] M. Di Mauro, F. Donato, G. Lamanna, D. A. Sanchez, and P. D. Serpico, Astrophys. J. **786**, 129 (2014).
[48] M. Ajello *et al.*, Astrophys. J. **800**, L27 (2015).
[49] F. W. Stecker, C. Done, M. H. Salamon, and P. Sommers, Phys. Rev. Lett. **66**, 2697 (1991); **69**, 2738(E) (1992).
[50] O. Kalashev, D. Semikoz, and I. Tkachev, JETP **147**, 3 (2015).
[51] K. Murase, Y. Inoue, and C. D. Dermer, Phys. Rev. D **90**, 023007 (2014).